C. R. Geoscience 349 (2017) 260–268

Contents lists available at ScienceDirect

Comptes Rendus Geoscience

www.sciencedirect.com

External Geophysics, Climate, and Environment

Sediment flocculation in the Mekong River estuary, Vietnam, an important driver of geomorphological changes

Nicolas Gratiot [a,b,c,*], Audrey Bildstein [c], Tran Tuan Anh [d], Heiko Thoss [d], Hervé Denis [a,b], Hervé Michallet [e], Heiko Apel [d]

[a] Université Grenoble Alpes, CNRS, IRD, Grenoble INP, IGE, 38000 Grenoble, France
[b] Institute of Engineering, Université Grenoble Alpes, 38000 Grenoble, France
[c] Centre asiatique de recherche sur l'eau (CARE), Bach Khoa University, VNU-HCM Ho Chi Minh City, Viet Nam
[d] GFZ German Research Centre for Geoscience, Section 5.4 Hydrology, 14473 Potsdam, Germany
[e] University Grenoble Alpes, CNRS, LEGI, CS40700, 38058 Grenoble, France

ARTICLE INFO

Article history:
Received 5 May 2017
Accepted after revision 14 September 2017

Handled by Isabelle Manighetti, Rutger De Wit, Stéphanie Duvail and Patrick Seyler

Keywords:
Floc
Settling velocity
Particle size
Mekong estuary
Coastal erosion

ABSTRACT

Over the past several decades, major hydro-sedimentary changes have occurred in both continental and coastal regions of the Mekong Delta, and this has severely impacted coastal erosion. A good characterization of floc properties and of their changes over time is necessary to gain comprehensive understanding and modelling of hydrodynamics and of the associated geomorphological changes. This paper quantifies the influence of sediment concentration, turbulence and differential particle settling on flocculation through field and laboratory investigations of the Mekong estuary. For concentrations lower than 200 $mg \cdot L^{-1}$, the particles do not exhibit a dynamic response to their environment, while for higher concentrations (up to 3–4 $g \cdot L^{-1}$), particle size and settling velocity increased by more than one order of magnitude. Flocculation by differential settling has not been sufficiently investigated yet, but this study reveals it as a predominant factor for siltation in quiescent environments such as the ones existing in the inner mangrove fringe. Such results are important to provide realistic simulations of the coastal evolution.

1. Introduction

The Mekong River originates in the Tibetan plateau of the Himalayas and flows across six countries (China, Myanmar, Lao PDR, Thailand, Cambodia, Vietnam) before finally discharging into the East Sea (South China Sea) through its vast plane delta (~60,000 km^2). About seventy million people live in the Mekong region and half of these people live within fifteen kilometers of the river's banks (MRC, 2011). Downstream, the Mekong Delta is home to about seventeen million people in Vietnam, and is often referred to as the rice-bowl of Southeast Asia due to its high agricultural productivity. Aquaculture and wild fishing also play important roles in the Vietnamese and Cambodian economies. One major factor for this high productivity is the annual large-scale flooding of the delta during the monsoon season, bringing both sufficient water and nutrient-rich sediments to the floodplains (Hung et al., 2012).

The Mekong basin has seen major transformation over the past few decades due to changes in land use (Valentin et al., 2008), construction of dams (Kondolf et al., 2014; Peteuil et al., 2014), and the mining of sand from the

* Corresponding author. Université Grenoble Alpes, CNRS, IRD, Grenoble INP, IGE, 38000 Grenoble, France.
E-mail address: nicolas.gratiot@ird.fr (N. Gratiot).

https://doi.org/10.1016/j.crte.2017.09.012
1631-0713/

riverbed for construction (Anthony et al., 2015; Bravard et al., 2013; Brunier et al., 2014). Climate change is also impacting sea levels and terrestrial runoff (Darby et al., 2016; Manh et al., 2015). All these processes have led to major hydro-sedimentary changes in terms of lower sediment conveyance and reduction of the quantity of particles that ultimately reach the estuarine and coastal waters. According to Loisel et al. (2014), reduction of suspended sediment concentrations (SSC) is now happening at a trend of 5% per year. According to Manh et al. (2015), total sediment delivery to the ocean could be reduced by as much as 95%, when compared to the 'pre-dam' era, if all projected dams are constructed. These transformations have already caused serious changes in the morphological development and stability of the delta, as reported by Anthony et al. (2015). While sediment conveyance has led to a net progradation (+16 m/y) of the delta over the last 3000 years, the 600-km-long shoreline is currently eroding at an unprecedented rate of −12 m/y (Anthony et al., 2015), with negative impacts on socio-economic activities, benthic habitats, and mangrove ecosystems.

The Mekong Delta's adaptation to ongoing changes in the coming decades will depend on a detailed understanding of how sediments are produced in the headwater catchments (Valentin et al., 2008), transported along stream and over the floodplains (Kondolf et al., 2014; Manh et al., 2014, 2015) and deposited along shore (Nowacki et al., 2015), and also how climate (Darby et al., 2016) and anthropogenic (Anthony et al., 2015) perturbations modify sediment fluxes from land to the ocean.

The physical properties of sediments transported in the Mekong River significantly contribute to the morphological evolution of the delta. At a microscopic scale, the main processes that ultimately control sediment dynamics are flocculation, floc breakage and hindered settling. Flocculation is the aggregation of primary particles (clay and silt) to form flocculi of a few microns, micro-flocs of some tens of microns, and macro-flocs of hundreds of microns (Lee et al., 2014). Flocculation is determined by a combination of physical (sediment concentration, turbulence, differential settling) and biological effects (Tran and Strom, 2017; Verney et al., 2009). The collision of particles due to different settling velocities is a well-identified process of flocculation (Hill et al., 1998; Lick et al., 1993), which has been poorly studied during the last decade. When fluvial waters discharge into the ocean, salinity becomes a driver of flocculation. Floc breakage is another important process for understanding sediment dynamics. It typically occurs when flocs migrate in regions with highly turbulent conditions. The collision and/or shearing then lead(s) to the disintegration of the most poorly bounded particles. A third important process is hindered settling, which is a process that corresponds to the decrease of the settling velocity of flocs when the concentration of particles (by volume) becomes high enough to enhance fluid viscosity. Flocs are then in strong interactions, which can lead to the stratification of the water column and the presence of lutocline, a sharp density interface that separates the suspended sediment layer on top and the fluid mud layer underneath. Sand particles, which do not flocculate, have a less complex behavior than flocs, as their transport is solely governed by hydraulic laws.

This study focuses on the characterization of the physical properties of suspended sediment in the estuarine area of the Mekong Delta, aiming to quantify the proportion of inert sand and cohesive particles (clay and silt) present in the water column and its change over tidal cycles. Since the initial work of Wolanski et al. (1996, 1998), there has been no follow-up on the characterization of recent estuarine floc properties. This paper aims to fill this lack by looking at how flocculation modifies sediment dynamics in the estuary. More precisely, we aim to characterize the respective influence of SSC, turbulence, and differential settling on the flocculation of particles. It is worth noting that the phase of settling conditions has long been recognized as important for flocculation (Curran et al., 2003; Gratiot and Anthony, 2016; Lick et al., 1993) and sedimentation, but has been poorly studied because of instrumental limitations. Thanks to the SCAF device (System for the Characterization of Aggregates and Flocs), it is now possible to measure the settling velocity of particles during their falling in a more direct and simple way (Gratiot et al., 2015).

This study is based on field surveys and laboratory investigations. We conducted two measurement campaigns during high and low Mekong water discharge in December 2015 and March 2016, respectively, to assess the natural variability of flocs and their dynamics. The laboratory experiments were dedicated to quantifying the respective influence of SSC, turbulence and differential settling on flocculation dynamics. Based on these field measurements and laboratory experiments, we analyzed the physical properties of the suspended sediment particles and quantified flocculation dynamics.

2. Material and methods

For a complete description of this section, please refer to the Appendix in the supplementary material.

We conducted the field surveys in one of the main branches of the Mekong estuary during both the high flow and low flow hydrological seasons in December 2015 and March 2016.

In each survey, we monitored hydrodynamic conditions and sampled the water from three cross sections (T1, upstream; T2, middle; T3, downstream), separated by distances of 10 and 15 km, respectively. The location of the transects was chosen to characterize saline water intrusion (Fig. 1). In total, 243 samples were collected at various depths and times. We selected fifteen of those samples, showing contrasted SSC and hydrodynamic conditions, for measuring in situ settling velocity experiments. The number of samples for this analysis had to be limited because of time constraints, as each settling experiment lasts at least five hours.

During the second survey, we also sampled 5 litres of fluid mud to carry out further JAR tank experiments in the laboratory to investigate the specific influence of SSC and turbulence on floc properties.

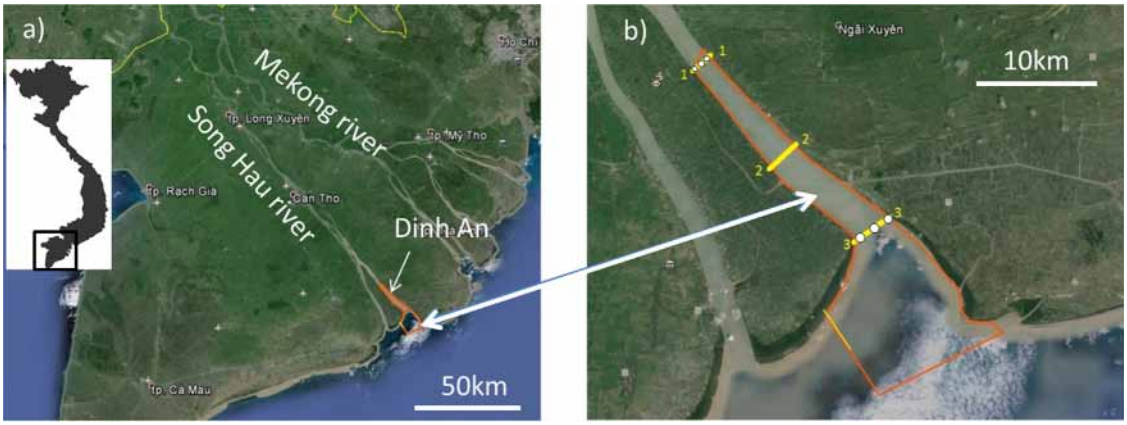

Fig. 1. a) Map of the lower Mekong Delta with b) focus on the Song Hau Estuary showing the three transects (T1, T2, T3) monitored during the field campaigns.

3. Results

3.1. Stratification of the water column and high suspended sediment concentration near the river bottom

Figs. 2a and 2b show vertical profiles of temperature (blue circles), salinity (blue dots), and SSC (black crosses) recorded on the right bank of the river at transects T1 and T3 during high tide in December 2015. It typically illustrates the vertical distribution of suspended sediment and stratification of the water column. Similar profiles were observed many times at both transects T1 and T3 during the two field surveys. The vertical profile of SSC shows a marked stratification, with jumps in SSC. These stratifications are lutoclines of which two (or three in Fig. 2b) can be observed. The first lutocline is found in the free-flowing water column and separates an upper layer, characterized by SSC values lower than 100 $mg{\cdot}L^{-1}$, from a layer with high SSC concentration reaching some hundreds of $mg{\cdot}L^{-1}$. In the profile shown in the left panel of Fig. 2a, lutocline 1 is at 8 m depth, in the right panel at 4 m. Lutocline 1 of T1 is typically associated with a halocline, where the salinity changes by steps, from about 0.8 near the surface to about 3.0 in the concentrated layer. Lutocline 1 of T3 is also associated with a halocline, but salinity changes from about 12 near the surface to about 25 in the concentrated layer (Fig. 2). This simultaneous evolution between SSC and salinity, observed in both transects, indicates that the lutocline is associated with the tidal-induced movement of the salt wedge in the estuary. It means that SSC dynamics is influenced by hydrodynamics (the change in flow) and the associated dynamics of salinity. There is no thermocline, as water temperature ranges from 30.3 °C near the surface to 30.15 °C in the concentrated layer. The vertical profiles of turbidity show the development of a second (or third in Fig. 2b) lutocline near the bottom of the river. Monitored SSC increases in a thin layer of several centimeters near the bottom, where values larger than 2.0 $g{\cdot}L^{-1}$ are found. This corresponds to an increase of about one order of magnitude compared to the SSC in the water column below lutocline 1. Although much larger SSC values were not recorded due to instrumental and practical constraints (the sensor of the probe does not reach the riverbed because of the protective cage and reaches saturation at 3000 NTU (which corresponds to 4.4 $g{\cdot}L^{-1}$), it can be expected that they reach tens or even hundreds of grams per liter, as observed in other muddy estuarine

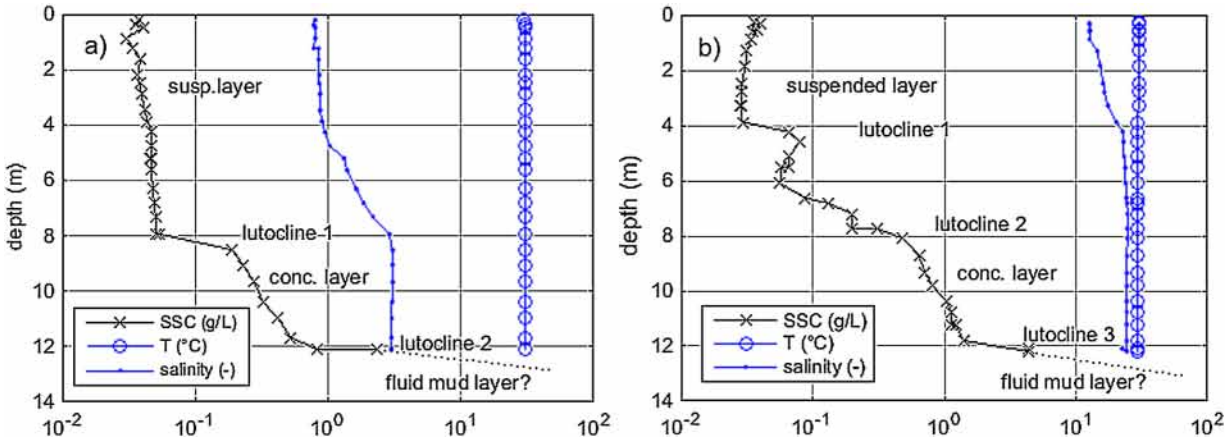

Fig. 2. Vertical stratification of the water column measured at a) transect T1 on 11th December 2015 at 17:30 local time; b) transect T3 on 10 December 2015 at 17:07 local time.

systems (Mehta, 1989; Sottolichio et al., 2011; Winterwerp, 2002). This near bed lutocline is not associated with a halocline or a thermocline.

To conclude, the vertical stratification shows that significant vertical gradients of turbidity and salinity exist in the water column. They result from the permanent interaction of fluvial and marine waters in the estuarine area, under the cyclic forcing of tides and the annual flood rhythm of the Mekong. We anticipate that this significant sediment dynamics modifies floc properties in the water column.

3.2. Influence of SSC on floc dynamics under turbulent dominated conditions

Fig. 3 synthesizes the 21 experiments conducted in the JAR tank under turbulent conditions and shows the mean diameters of the particle populations (flocculi, micro-flocs, and macro-flocs). Fig. 3a corresponds to natural samples before sonication. It is worth noting that the 300–500 mg·L^{-1} range of SSCs appeared to play a key role for floc dynamics: for lower concentrations, the two water sediment mixtures that were characterized contained a single class of particles that corresponds to very fine silt (flocculi). Above 300–500 mg·L^{-1}, water sediment mixtures were systematically composed of two populations, as the example presents in Figs. 3b and 3c. The fine silt population exhibited a mean particle diameter in the range of [7–12.5] ± 10% μm, while the coarser population had a mean particle diameter in the range of [112–310] ± 10% μm. The fine silt population predominated in volume and constituted 83 to 94% of the total volume, without evidence of changes in the proportion of small and coarse sub-populations with increasing SSC. For both small and coarse-sized populations and for all runs conducted beyond 900 ± 40 mg·L^{-1} to 99,000 ± 5000 mg·L^{-1}, the mean floc diameter remained constant. Fig. 3c shows the PSD of particles for the same samples as those presented in Fig. 3a, but after two minutes of sonication. For all runs, sonication led to the apparition of a third population of particles characterized by a mean diameter in the range of 1.8–4.0 ± 10% μm. The second population (by increasing size) had a geometric mean diameter in the range of 6.3–12.2 ± 10% μm that was partially superimposed with the population of very fine particles observed before sonication (circles in Fig. 3a). The coarse class of particles had a geometric mean diameter in the range of 15–65 ± 10% μm, which was far below the geometric mean particle diameter measured before sonication (squares in Fig. 3a).

As shown in Figs. 3a and 3c, the particle size is systematically reduced after sonication, which confirms that the samples were constituted of cohesive sediments and not of sand particles. For 95% of samples, macro flocs and flocculi were broken up to form micro-flocs, flocculi, and primary particlesFigs. 3b and 3d. The discontinuous distributions of floc populations after sonication (Fig. 3c) support the interpretation that the flocs were destroyed, rather than reduced in size by abrasion. Following this interpretation, the breakdown of flocs resulted in macro-flocs breaking into micro-flocs, flocculi, and primary particles.

Fig. 4 shows the principal characteristics of floc populations for both laboratory (left panels) and field (right panels) measurements. The variation of PSD with concentration, as measured in the field (Figs. 4b and 4d), shows the same flocculation characteristics as seen in the laboratory experiments (Figs. 4a and 4c). In particular, the existence of a unimodal distribution can be observed for SSC values lower than 200 mg·L^{-1}, a transition zone between 200 and 500 mg·L^{-1}, where unimodal and bimodal distributions coexist, and bimodal distributions for higher concentrations. We note that the size of macro-flocs and flocculi do not increase with SSC. Results from field and laboratory experiments, presented in Fig. 4, show that flocculi are the dominant particle population (80–100%). It is also interesting to note that the particle size is slightly larger for the field samples (geometric mean D_p = 15 μm) than for the laboratory samples (geometric mean D_p = 10 μm). This point is further elaborated in the discussion section.

The results presented in Figs. 3 and 4 are in qualitative agreement with the PSD reported by Wolanski et al. (1996, 1998). For varying conditions of tide and hydrological flows, these authors measured median particle sizes in the range of 30–80 μm. By applying the separation technique of Launay (2014), we can go beyond the previous analysis and provide statistics of particle diameters and total volume of each population (see the electronic supplements for further details).

3.3. Influence of SSC on floc dynamics under quiescent and settling dominated conditions

The sedimentation of particles was characterized in a SCAF settling tube. It is an optical settling column that provides two different settling velocities (Gratiot et al., 2015; Wendling et al., 2015; electronic supplements): $w_{s,q}$

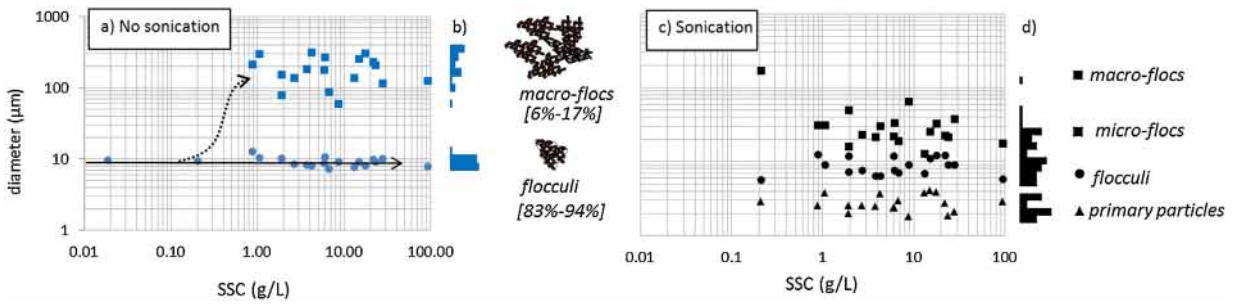

Fig. 3. Variation of the mean particle diameter with suspended sediment concentration for (a) unsonicated and (c) sonicated samples. Each symbol refers to a specific sub-population measured from the PSDs in Fig. 3. In Fig. 3a, the dotted line with the arrow indicates the formation of flocs (micro and macro flocs with threshold at 150 μm) for concentrations beyond 900 mg·L^{-1}; (b) and (d): histogram distribution of the points represented in panels a) and c).

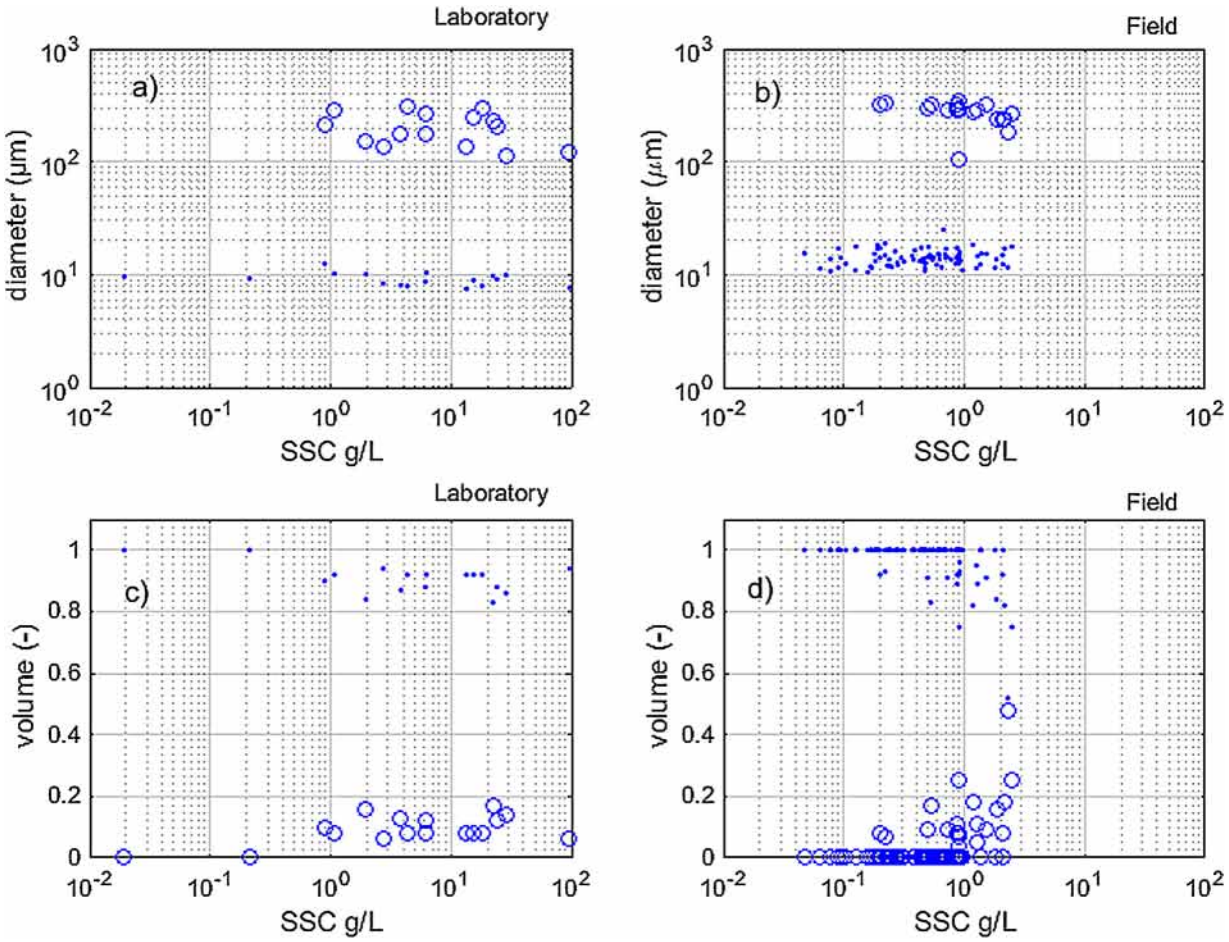

Fig. 4. Intercomparison of particle size and floc characteristics for laboratory (a and c) and field (b and d) samples under turbulent dominated conditions. (a) and (b): variation of the mean particle diameter with SSC. If, for the same SSC, a circle and a dot are shown, two sub-populations of particle sizes exist (bimodal particle size distribution); (c) and (d): variation of the volumetric partition between flocculi (dots) and macro-flocs (circles) for increasing SSC values.

corresponds to the velocity when particles are settling in a fluid at rest (quiescent conditions); $w_{s,\neq}$, corresponds to the increased velocity when particles have been flocculating together by differential settling. Fig. 5a compiles results from all experiments conducted under quiescent ($w_{s,q}$) and settling ($w_{s,\neq}$) conditions. For both conditions, the variation of settling velocity with SSC shows a similar pattern.

At low concentrations ($SSC < 200\ mg{\cdot}L^{-1}$), a free settling regime develops. Particles settle without any interactions with other settling particles. This regime is characterized by a constant and very low settling velocity ($w_{s,q} \sim 10^{-5}\ m{\cdot}s^{-1}$ and $w_{s,\neq} \sim 2{\cdot}10^{-5}\ m{\cdot}s^{-1}$). For higher concentrations ($200\ mg{\cdot}L^{-1} < SSC < 3.0\ g{\cdot}L^{-1}$), settling velocity increases to reach maximal values of $w_{s,q} \sim 1.8{\cdot}10^{-3}\ m{\cdot}s^{-1}$ and $w_{s,\neq} \sim 6.3{\cdot}10^{-4}\ m{\cdot}s^{-1}$ for concentrations of 2.7 and $4.3\ g{\cdot}L^{-1}$, respectively. Beyond $SSC \sim 5.0\ g{\cdot}L^{-1}$, the hindered process becomes predominant and settling velocity decreases significantly with SSC. Flocs reach higher volumetric concentration for lower mass concentrations when flocculation is reinforced by differential settling. As a direct consequence, the hindered regime is observed to start at a lower SSC value ($2.7\ g{\cdot}L^{-1}$) than without flocculation by differential settling ($4.3\ g{\cdot}L^{-1}$). It is worth noting that for the highest concentrations tested, $SSC = 99 \pm 5\ g{\cdot}L^{-1}$, settling velocity is still ten times higher than the value observed in the free settling regime. This point will be further discussed in Section 4.

The experimental curves of $w_{s,q}(SSC)$ and $w_{s,\neq}(SSC)$ are well described by a semi empirical law of the form (Hwang and Mehta, 1989):

$$w_s = \begin{cases} w_{s\,free} & SSC < C_1 \\ a\dfrac{SSC^n}{\left(SSC^2 + b^2\right)^m} & C_1 < SSC < C_{gel} \end{cases} \quad (1)$$

where

$w_{s,free}$ ($m{\cdot}s^{-1}$): free settling velocity

a: velocity scale coefficient

n: flocculation settling exponent

b: hindered settling coefficient

m: hindered settling exponent and

C_1, C_{gel}: zone concentration limits between free regime and flocculation regime, and hindered regime and consolidation regime, respectively.

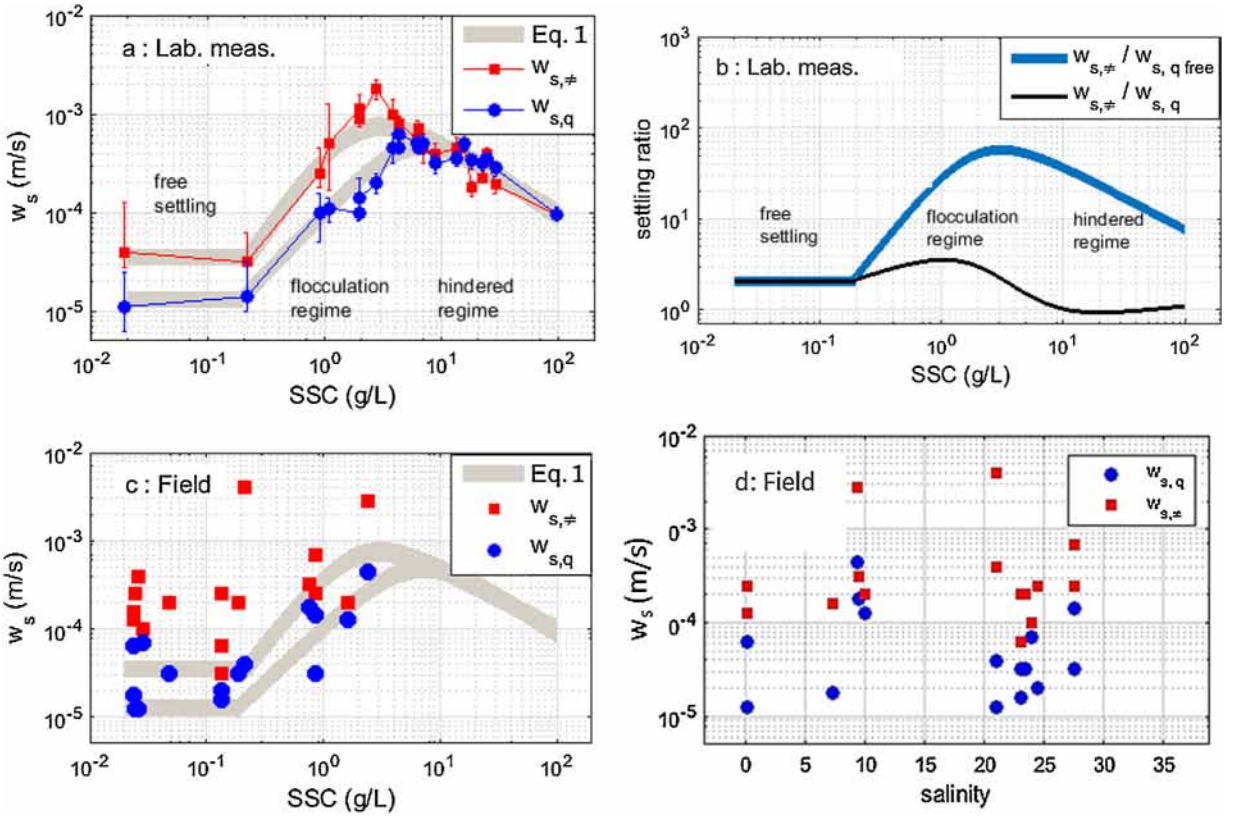

Fig. 5. (a) Variation in the settling velocity of particles with suspended sediment concentration for (a) laboratory conditions. The squares and circles correspond to settling velocity under quiescent and settling conditions, respectively. The grey lines correspond to interpolated settling laws according to Hwang and Mehta (1989); (b): respective effect of differential settling and flocculation + differential settling on flocculation. (c) Settling velocity measured in the field. The grey lines are reported from Fig. 5a; (d): effect of salinity on the settling velocity of particles in the field.

The parameterization of a, n, b, m and C_1 was done by trial and error; fitting parameters are reported in the Supplementary Material. In our case, the gelling concentration (i.e. the concentration beyond which a loose soil structure develops) was not reached (beyond 99.0 g·L^{-1}). It typically appears when particles are deposited in the bed and start compacting.

Fig. 5b shows the ratio between $w_{s,\neq}$, $w_{s,q}$, as deduced from Eq. (1). The black curve illustrates the unique effect of flocculation by differential settling, while the blue curve represents the cumulative effects of concentration and differential settling. In the free regime, flocculation by differential settling accelerated the settling of particles by nearly two-fold. This ratio increases to 3.5 when SSC = 1.0 g·L^{-1}; the effect of flocculation by differential settling then reduces and tends to zero ($w_{s,\neq}/w_{s,q} = 1$) in the hindered regime. The cumulative effect of flocculation by concentration and differential settling is very strong (blue curve). The maximum settling velocity was as high as $1.8{\cdot}10^{-3}$ m·s^{-1} for SSC = 2.7 ± 0.2 g·L^{-1}, i.e. an increase of two orders of magnitude as compared to the settling velocity of flocculi in quiescent conditions in the free regime. For SSC values in the range of 2–5 g·L^{-1}, the ratio between $w_{s,\neq}$ and $w_{s,q\ free}$ is higher than 50.

Fig. 5c compares field and laboratory measurements. Both show similar patterns but the field data are more dispersed. For suspended concentrations below 200 mg·L^{-1}, the settling velocity is constant for both quiescent and differential settling regimes. For higher concentrations, settling velocity increases because of the flocculation of particles. The maximum settling velocity is obtained for the highest SSCs sampled (SSC = 2.4 ± 0.2 g·L^{-1}) and reaches a value as high as $w_{s,q} \sim 4.5{\cdot}10^{-4}$ m·s^{-1} and $w_{s,\neq} \sim 2.8{\cdot}10^{-3}$ m·s^{-1}. The floc settling velocity values estimated in the field were systematically higher than the ones obtained in the laboratory. Furthermore, under field conditions, it was not possible to explore the hindered regime because of technical limitations for sampling. The highest SSC values are observed in a thin layer near the riverbed, which cannot be sampled in the field (see Fig. 2).

Fig. 5d investigates whether salinity affects the settling velocity in the field measurements. Contrary to the laboratory experiments, where the salinity was fixed (S = 17), the salinity during the field measurements varied markedly along the vertical and longitudinal directions (see Figs. 2a and 2b), but also with the tidal cycle. However, Fig. 5d does not show any clear relation between salinity and settling velocity, which differs from the observations of Kumar et al. (2010). This may be due to an important co-variation of salinity with other hydrodynamic and biogeochemical factors during the tidal cycle. For example, the intrusion of saline water during floods also coincides with the resuspension of sediments from the riverbed and

high levels of turbulence. Salinity, sediment concentration and turbulence are three drivers of flocculation and deflocculation that vary simultaneously, so that their respective effects can barely be identified from field measurements. However, it can be hypothesized that the different salinity levels are at least partly responsible for the spread of the settling velocities for the field samples shown in Fig. 5c, particularly at low SSC.

4. Discussion and conclusions

Our first objective in this study was to characterize whether particles transported in the water column were inert (sand) or cohesive (clay, flocculi and flocs). For the whole set of suspended sediment samples collected during two field campaigns in the high and low flow season (243 samples), we found that cohesive sediment was predominant. Analysis of the particle size distributions at no point showed the existence of sand in suspension. This was demonstrated by PSD measurements before and after sonication, which destroys any flocs present in the samples. While some samples had PSDs with sub-populations peaking around 120–300 μm, i.e. in the range of sand particles, all of them were transformed by sonication into smaller particles. This indicates that sand is not present in suspension in the Mekong estuary. However, it must be noted that sand was occasionally found in bottom sediment samples from the riverbed, indicating the presence of sand on the riverbed. Moreover, transport of sand along the bed is indicated by the occurrence of sand bars located outside the estuary on the verge to the open ocean.

Our second objective was to characterize the respective impacts of sediment concentration and turbulence level on the flocculation process. The major results we obtained are:

- PSDs systematically exhibited a unimodal population of flocculi for sediment concentrations below 200–300 $mg{\cdot}L^{-1}$ in turbulent conditions. For higher concentrations, the flocculation process led to the formation of macro-flocs with diameters in the range of $150 \leq D_p \leq 300$ μm, i.e. fifteen times larger than the mean diameter of the flocculi population ($8.0 \leq D_p \leq 20.0$ μm). These macro-flocs contribute to a significant increase of sediment settling flux because of their large size, even if they account for less than 20% of the total sediment volume (Figs. 4c and 4d);

  Interestingly, the variation of flocculation with SSC was observed to be rather discontinuous, with the most notable changes occurring between 200 and 500 $mg{\cdot}L^{-1}$ (Fig. 4). Beyond this range of concentration, the macro-floc sub-population was quite stable in both size and volume. For higher SSCs, floc growth was assumed to be limited by turbulence, as described by Dyer (1989) and Kranenburg (1994).
- In quiescent conditions, a free settling regime developed for low concentrations (SSC < 200 $mg{\cdot}L^{-1}$). In this regime, the flocculi were predominant and settled down independently. The measured settling velocity seemed to be independent of the SSC and very small ($w_{s,q} < 8.0{\cdot}10^{-5}$ $m{\cdot}s^{-1}$ in the field and $w_{s,q} < 1.5{\cdot}10^{-5}$ $m{\cdot}s^{-1}$ in the laboratory). From 200 to 3000 $mg{\cdot}L^{-1}$, flocculation occurred and increased the settling velocity, reaching values as high as $6.0{\cdot}10^{-4}$ $m{\cdot}s^{-1}$, i.e. an almost eight-fold increase when compared with the settling rate for low concentrations. We observed an acceleration of the velocity of particles during their settling, which underlined the role of differential settling on flocculation. Under these conditions, settling velocity reached values as high as $3.0{\cdot}10^{-3}$ $m{\cdot}s^{-1}$, i.e. a 100-fold increase as compared to settling for low concentrations. This behavior differs from the conclusions of Dyer (1989), who depicted an abrupt decrease of flocculation when turbulence tends to zero. Instead, our observations validate the expectation of Manning and Dyer (1999, fig. 14 in their paper) and of Curran et al. (2003), who proposed an accelerated flocculation for quiescent conditions ($G \sim 0\ s^{-1}$). Finally, it is worth noting that for the 16 measurements performed in the field, the increase of settling velocity attributed to differential settling was always significant. It increases the settling velocity by 20 to 2500% when compared to conditions without flocculation by differential settling.

The examination of field and laboratory data shows that flocculation was found to be systematically higher *in situ* than in the laboratory (Fig. 4 and Fig. 5). A first explanation might relate to the experimental device. It is believed that the high level of turbulence ($G \sim 44\ s^{-1}$) required to maintain the largest flocs in suspension in the jar tank may have limited their growth, inertial forces of eddies overpassing binding forces, as described by Kranenburg (1994). Another hypothesis might relate to the nature of the particles. Estuarine areas are known to be catalyzers of biogeochemical processes, and biological activity often has an important effect on floc dynamics (Mari et al., 2012; Verney et al., 2009). We cannot exclude that storage conditions in the dark tank at 6 °C during transportation into the laboratory had altered the organic matter and reduced its ability to flocculate. Despite this slight difference between floc properties in the field and in the laboratory, the experimental conditions offered the possibility to explore a wider range of concentrations (from 20 $mg{\cdot}L^{-1}$ to 99,000 $mg{\cdot}L^{-1}$) and regimes (free, flocculated, hindered) than in the field.

A global comparison of our experiments with those in the literature is presented in Fig. 6. This figure shows the reactive nature of flocculation in the natural Mekong River estuarine fluid mud determined in this study compared to a large range of other mud settings. Before comparing the data, it must be kept in mind that the various techniques used in prior studies can generate inherently different results (along the *Y* axis), as suggested by Ross (1988). Furthermore, most prior experiments focused on the flocculation regime (experiments 1 to 18) and only five studies covered the full range of settling regimes, up to the hindered regime (experiments 19 to 23). However, the comparison shows that the floc characteristics of the Mekong Estuary (present study, No. 23, circles) have several specificities.

For SSC ≤ 200 $mg{\cdot}L^{-1}$, the characteristics of flocculi in the Mekong River are not influenced by sediment concentration; the settling velocity seems to remain

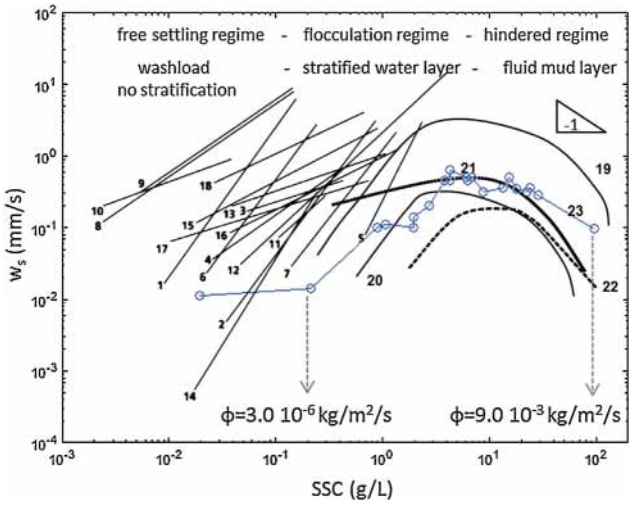

Fig. 6. Regression curves showing the variation of settling velocity with suspended sediment concentrations obtained by various authors from field experiments for a range of temperate estuaries and bays (adapted and completed from Pejrup and Mikkelsen (2010) and Gratiot and Anthony (2016)), and from the Mekong river mouth (circles, present study). The location of sites reported in the figure (Nos. 1 to 23) are given in the electronic supplements.

constant, which is unique for the 23 available datasets (Fig. 6). Comparably, the settling velocities in the Mekong estuary were relatively low, which may be attributed to the characteristics of their flocs and the signature of the upstream fluvial environment. The existence of this free settling regime implies that floc characteristics in the water column can be adequately modelled with a single class of flocculi particles (D_f in the range of 8–20 μm and w_s in the range of $1–8{\cdot}10^{-5}$ m·s^{-1}) as long as $SSC \leq 200$ mg·L^{-1}. Because settling velocity is very low for this range of concentration ($1–2{\cdot}10^{-5}$ m·s^{-1}), we may expect a homogeneous distribution of SSC over the water column (washload regime with no stratification).

For 200 mg·L^{-1} < SSC < 2–6 g·L^{-1}, settling velocity increases quite linearly with SSC. The modification of floc characteristics in this range of concentration is similar to that observed in other rivers and estuaries worldwide.

For SSC > 2–6 g·L^{-1}, settling velocity decreases with SSC; this is characteristic of the hindered regime. This decrease is rather gentle, with the direct consequence that in the Mekong Delta the sediment settling flux $\varphi = w_s$ x SSC increases even for concentrations up to SSC = 99.0 g·L^{-1}. In contrast to this, the sediment settling flux starts to decrease for SSC values beyond 30 g·L^{-1} for all other rivers and estuarine environments reported in Fig. 6.

All floc series presented in Fig. 6 were obtained under quiescent conditions. The corresponding sediment settling flux can tentatively be linked with the observed coastal geomorphic processes at regional scale, bearing in mind that sediment settling flux under quiescent conditions can significantly differ from those under turbulent conditions (Gratiot et al., 2005; Sottolichio et al., 2011). The sediment settling flux $\varphi = w_s$ x SSC that can be deduced from Eq. (1) is about $\varphi = 10^{-7}–10^{-6}$ kg·m^{-2}·s^{-1} at low concentrations and increases up to $6.0–9.0{\cdot}10^{-3}$ kg·m^{-2}·s^{-1} in the hindered regime, when SSC values exceed 30 g·L^{-1} (Fig. 6). In terms of geomorphic structuration, this large difference (> 10^3) between settling fluxes at low and high concentrations, clearly puts the focus on the fluid mud layer (very high concentration and hindered regime) as a driver of siltation and coastal changes. Even if the fluid mud layer is thin and confined to a few centimeters near the bottom of the river, its existence might enhance sediment settling flux and lead to local siltation and mud accretion rather than longshore transport.

At the scale of the Mekong Delta, particles are expected to be mainly transported as washload within the river flow. Inland SSC rarely exceeds 200 mg L^{-1}, which corresponds to the free settling regime with low settling velocity. Upon their arrival into the delta distributary mouths, the combined effects of the saline gradient and the tidal mixing of fluvial and oceanic waters enhance flocculation and induce water stratification (Fig. 2). Along the surrounding creek and mangrove fringes, the lower turbulence conditions offer favorable conditions to initiate flocculation by differential settling. Then, sediments will be most likely trapped locally because the Mekong sediment settling flux φ is very high. When compared to the other two tropical environments with available data (Tampa bay, Florida, No. 20 and Kaw river mouth, French Guiana, No. 22, in Fig. 6), the sediment settling flux φ is at least one order of magnitude higher for SSC > 100 g·L^{-1}.

The assumption of a local trapping in the delta distributary mouths region of the Mekong Estuary is sustained by the observed geomorphic changes described by Anthony et al. (2015, fig. 3 of their paper). Based on a satellite survey of shoreline changes, they observed that the bed load sediment transport and deposition in the delta distributary mouths is in balance with erosion, while the coastal regions of the Mekong Delta located further away from the river mouths has been eroding at an unprecedented mean rate of 20–25 m/y. In forthcoming decades, we may expect that floc properties ensure the trapping of sediment in river mouths and that erosion will pursue in the coastal regions. However, coastal erosion cannot be explained by SSC dynamics alone. The

bed transport of sand plays another important role for this (Brunier et al., 2014).

Acknowledgments

J. Némery and T. Phong are fully acknowledged for their kind help during the preliminary experiments; we also would like to acknowledge all colleagues involved in the field survey. This project was partially funded by the "Institut de recherche pour le développement", GFZ German Research Centre for Geoscience, as well as ANR SCAF JCJC ANR-12-JS06-0006 project and LMDCZ (EU-AFD-SIWRR) projects. A scholarship funding by the German Academic Exchange Service DAAD (NAWAM program, No. 91587027) of the PhD work of Tran Tuan Anh is gratefully acknowledged. We would like to thank the two reviewers, K. Strom and R. de Wit (invited associated editor), as well as the associated editor I. Manighetti for their fruitful and constructive remarks. M. Marchesiello is acknowledged for her support to improve the English. H. Paquet is acknowledged for proof reading.

Appendix A. Supplementary data

Supplementary data associated with this article can be found, in the online version, at http://dx.doi.org/10.1016/j.crte.2017.09.012.

References

Anthony, E.J., Brunier, G., Besset, M., Goichot, M., Dussouillez, P., Nguyen, V.L., 2015. Linking rapid erosion of the Mekong River delta to human activities. Sci. Rep. 5 (2015), 14745.

Bravard, J.-P., Goichot, M., Gaillot, S., 2013. Geography of sand and gravel mining in the Lower Mekong River. First survey and impact assessment. Echogeo 26, 2–18.

Brunier, G., Anthony, E.J., Goichot, M., Provansal, M., Dussouillez, P., 2014. Recent morphological changes in the Mekong and Bassac river channels, Mekong Delta: the marked impact of river-bed mining and implications for delta destabilisation. Geomorphology 224, 177–191.

Curran, K.J., Hill, P.S., Milligan, T.G., 2003. Time variation of floc properties in a settling column. J. Sea Res. 49, 1–9.

Darby, S.E., Hackney, C.R., Leyland, J., Kummu, M., Lauri, H., Parsons, D.R., Best, J.L., Nicholas, A.P., Aalto, R., 2016. Fluvial sediment supply to a mega-delta reduced by shifting tropical-cyclone activity. Nature 539 (7628), 276.

Dyer, K.R., 1989. Sediment processes in estuaries: future research requirements. J. Geophys. Res. Oceans 94 (C10), 14327–14339.

Gratiot, N., Anthony, E.J., 2016. Role of flocculation and settling processes in development of the mangrove-colonized, Amazon-influenced mud-bank coast of South America. Marine Geol. 373, 1–10.

Gratiot, N., Michallet, H., Mory, M., 2005. On the determination of the settling flux of cohesive sediments in a turbulent fluid. J. Geophys. Res. Oceans 110 (C6), C06004.

Gratiot, N., Coulaud, C., Legout, C., Mercier, B., Mora, H., Wendling, V., 2015. Unit for measuring the falling speed of particles in suspension in a fluid and device comprising at least one measuring unit and one automatic sampler. (Patent-Publication number WO2015055963 A1).

Hill, P.S., Syvitski, J.P., Cowan, E.A., Powell, R.D., 1998. In situ observations of floc settling velocities. Marine Geol. 145, 85–94.

Hung, N.N., Delgado, J.M., Tri, V.K., Hung, L.M., Merz, B., Bárdossy, A., Apel, H., 2012. Floodplain hydrology of the Mekong Delta, Vietnam. Hydrol. Proc. 26, 674–686.

Hwang, K.-N., Mehta, A.J., 1989. Fine sediment erodibility in Lake Okeechobee, Florida. Report ufl/coel-89/019. Department of Coastal and Oceanographic Engineering, University of Florida.

Kranenburg, C., 1994. The fractal structure of cohesive sediment aggregates. Estuar. Coast Shelf S. 39, 451–460.

Kondolf, G.M., Rubin, Z.K., Minear, J.T., 2014. Dams on the Mekong: cumulative sediment starvation. Water Resour. Res. 50, 5158–5169.

Kumar, R.G., Strom, K.B., Keyvani, A., 2010. Floc properties and settling velocity of San Jacinto estuary mud under variable shear and salinity conditions. Cont. Shelf Res 30, 2067–2081.

Launay, M., 2014. Flux de matières en suspension, de mercure et de PCB particulaires dans le Rhône, du Léman à la Méditerranée. , PhD thesis. 434 p.

Lee, B.J., Toorman, E., Fettweis, M., 2014. Multimodal particle size distributions of fine-grained sediments: mathematical modeling and field investigation. Ocean Dynam. 64, 429–441.

Lick, W., Huang, H., Jepsen, R., 1993. Flocculation of fine-grained sediments due to differential settling. J. Geophys. Res. - Oceans. 98 (C6) 10,279-10,288.

Loisel, H., Mangin, A., Vantrepotte, V., Dessailly, D., Dat, D.N., Gaernesson, P., Ouillon, S., Lefebvre, J.-P., Mériaux, X., Thu, P.M., 2014. Analysis of the SPM concentration variability of the coastal waters under the Mekong's influence. Rem. Sens. Envt. 150, 218–230.

Manh, N.V., Dung, N.V., Hung, N.N., Merz, B., Apel, H., 2014. Large-scale suspended sediment transport and sediment deposition in the Mekong delta. HESS 18, 3033–3053.

Manh, et al., 2015. Future sediment dynamics in the Mekong delta floodplains: Impacts of hydropower development, climate change and sea level rise. Global Planet. Change 127, 22–33.

Manning, A.J., Dyer, K.R., 1999. A laboratory examination of floc characteristics with regard to turbulent shearing. Marine Geol. 160, 146–170.

Mari, X., Torréton, J.-P., Bich-Thuy Trinh, C., Bouvier, T., Thuoc, C.V., Lefebvre, J.-P., Ouillon, S., 2012. Aggregation dynamics along a salinity gradient in the Bach Dang estuary, North Vietnam. Estuar. Coast. Shelf Sci. 96, 151–158.

Mehta, A.H., 1989. On estuarine cohesive sediment suspension behavior. J. Geophys. Res. Oceans 94 (C10), 14303–14314.

MRC, 2011. Mekong River Comm. (MRC), 1 (Main Report), 2011, 254 p. Basin Development Plan Programme, Phase 2: Assessment of Basin-wide Development Scenarios. (Accessed: 2 May 2017)http://www.mrcmekong.org/assets/Publications/basin-reports/BDP-Assessment-of-Basin-wide-Dev-Scenarios-2011.pdf.

Nowacki, D.J., Ogston, A.S., Nittrouer, C.A., Fricke, A.T., Tri, V.P.D., 2015. Sediment dynamics in the lower Mekong river: transition from tidal river to estuary. J. Geophys. Res. Oceans 120, 6363–6383.

Pejrup, M., Mikkelsen, O.E., 2010. Factors controlling the field settling velocity of cohesive sediment in estuaries. Estuar. Coast. Shelf Sci. 87, 177–185.

Peteuil, C., Frétaud, T., Wirz, C., Camenen, B., Guertault, L., Le Coz, J., Dramais, G., 2014. In: Importance of field observation for managing sediment fluxes in hydropower projects design and operation. Proceedings of the 19th IAHR-APD Congress, Hanoi, Vietnam, 8 p.

Ross, M.A., 1988. Vertical structure of estuarine fine sediment suspensions. Technical Report. Coastal and Oceanographic Engineering Department, University of Florida, Gainesville.

Sottolichio, A., Hurther, D., Gratiot, N., Bretel, P., 2011. Acoustic turbulence measurements of near-bed suspended sediment dynamics in highly turbid waters of a macrotidal estuary. Cont. Shelf Res. 31, S36–S49.

Tran, D., Strom, K., 2017. Suspended clays and silts: are they independent or dependent fractions when it comes to settling in a turbulent suspension? Cont. Shelf Res. 138, 81–94.

Valentin, C., Agus, F., Alamban, R., Bricquet, J.-P, Chaplot, V., de Guzman, T., de Rouw, A., Janeau, J.-L., Orange, D., Phachomphonh, K., Duy Phai, D., Podwojewski, P., Ribolzi, O., Silvaera, N., Subagyono, K., Thiébaux, J.-P., Toan, T.D., Vadari, T., 2008. Runoff and sediment losses from 27 upland catchments in Southeast Asia: impact of rapid land use changes and conservation practices. Agric. Ecosyst. Environ. 128 (4), 225–238.

Verney, R., Lafite, R., Brun-Cottan, J.C., 2009. Flocculation potential of estuarine particles: the importance of environmental factors and of the spatial and seasonal variability of suspended particulate matter. Estuar. Coast. 32, 678–693.

Wendling, V., Gratiot, N., Legout, C., Droppo, I.G., Coulaud, C., Mercier, B., 2015. Using an optical settling column to assess suspension characteristics within the free, flocculation and hindered settling regimes. J. Soils Sediment 15, 1991–2003.

Winterwerp, J.C., 2002. On the flocculation and settling of estuarine mud. Cont. Shelf Res. 22, 1339–1360.

Wolanski, E., Ngoc Huan, N., Trong Dao, L., Huu Nhan, N., Ngoc Thuy, N., 1996. Fine-sediment Dynamics in the Mekong River Estuary, Vietnam. Estuar. Coast. Shelf Sci. 43, 565–582.

Wolanski, E., Nhan, N.H., Spagnol, S., 1998. Sediment dynamics during low flow conditions in the Mekong river estuary. Vietnam. J. Coastal Res. 14 (2), 472–482.